

Abundant anti-apoptotic BCL-2 is a molecular target in leukaemias with t(4;11) translocation

Blaine W. Robinson,¹ Kathryn C. Behling,¹ Manish Gupta,² Alena Y. Zhang,¹ Jonni S. Moore,³ Andrew D. Bantly,³ Cheryl L. Willman,^{4,5} Andrew J. Carroll,⁶ Peter C. Adamson,^{1,2,7} Jeffrey S. Barrett^{2,7} and Carolyn A. Felix^{1,7}

Divisions of ¹Oncology and ²Clinical Pharmacology & Therapeutics, The Children's Hospital of Philadelphia, Philadelphia, PA, ³Departments of Pathology and Laboratory Medicine, University of Pennsylvania School of Medicine, Philadelphia, PA, ⁴Department of Pathology and ⁵The Cancer Research and Treatment Center, University of New Mexico, Albuquerque, NM, ⁶Department of Genetics, University of Alabama at Birmingham, Birmingham, AL, and ⁷Department of Pediatrics, University of Pennsylvania School of Medicine, Philadelphia, PA, USA

Received 22 October 2007; accepted 15 January 2008

Correspondence: Carolyn A. Felix, MD, Division of Oncology, Leonard and Madlyn Abramson Pediatric Research Center, Room 902B, The Children's Hospital of Philadelphia, 3615 Civic Center Blvd., Philadelphia, PA 19104-4318, USA. E-mail: felix@email.chop.edu

Most infant acute leukaemias are characterized by *MLL* translocations, which are poor prognostic features with adverse effects on response to treatment (Pui *et al*, 2002). In particular, cases with t(4;11), the most common *MLL* translocation in acute lymphoblastic leukaemia (ALL), often are resistant to common anti-leukaemia cytotoxic drugs (Pieters *et al*, 1998). Infants also are more vulnerable to regimen-related toxicities, and more intensive treatment for infant ALL has increased both anti-leukaemia efficacy and treatment complications without improving outcome (Hilden *et al*, 2006). Although none have yet been utilized, any agent that increases sensitivity to anti-leukaemia cytotoxic drugs would be especially desirable for infant acute leukaemias because chemotherapy resistance and toxic deaths contribute to poor outcome (Reaman *et al*, 1985, 1999; Reaman, 2003; Hilden *et al*, 2006). The t(4;11) is also a

Summary

Chemotherapy resistance from imbalanced apoptosis regulation may contribute to poor outcome in leukaemias with t(4;11). Anti-apoptotic BCL-2 expression and target modulation were characterized in cell lines with t(4;11) and BCL-2 expression was examined in *MLL* and non-*MLL* infant/paediatric leukaemia cases by Western blot analysis and/or real-time polymerase chain reaction. Cytotoxicity of GenasenseTM (Oblimersen Sodium, G3139) alone or combined with cytotoxic drugs was assessed by MTT [(3-4,5-dimethylthiazol-2-yl)-2,5-diphenyl tetrazolium bromide] assays of the cell lines, applying pharmacostatistical response surface modelling of drug interactions. Apoptosis and cell cycle were evaluated by flow cytometry in RS4:11 cells. Primary leukaemias and cell lines with t(4;11) expressed abundant *BCL2* mRNA and protein. Variable, sometimes substantial *BCL2* mRNA was detected in other leukaemia subtypes. G3139 reduced *BCL2* mRNA and protein in RS4:11 cells. The most sensitive cell line to single-agent G3139 was RS4:11. Low G3139 concentrations sensitized RS4:11 and MV4-11 cells to select anti-leukaemia cytotoxic drugs. In RS4:11 cells, combining G3139 with doxorubicin (ADR) increased active caspase 3 and TUNEL staining compared to ADR alone, indicating greater apoptosis, and G3139 increased S-phase progression. The abundant BCL-2 affords a molecular target in leukaemias with t(4;11). G3139 exhibits preclinical activity and synergy with select cytotoxic agents in RS4:11 and MV4-11 cells, and these effects occur through apoptosis.

Keywords: GenasenseTM, apoptosis, leukaemia, BCL-2, infant.

high-risk feature in ALL in children where it occurs less often (Pui *et al*, 2004).

Interactions of specific pro- and anti-apoptotic BCL-2 family proteins in the intrinsic (mitochondrial) cell death pathway determine the apoptosis threshold and impact chemosensitivity and resistance (Nicholson, 2000; Certo *et al*, 2006; Letai & Scorrano, 2006). The cardinal anti-apoptotic regulator in this pathway, BCL-2, has a general role in chemotherapy resistance. However, many BCL-2 family members with opposing pro- or anti-apoptotic actions regulate apoptosis by forming homo- and heterotypic dimers (Reed *et al*, 1996; Nicholson, 2000; Danial & Korsmeyer, 2004) and, more recently, it was suggested that apoptosis deregulation in cancer is cell-type specific (Certo *et al*, 2006). BCL-2 family members are divided into three classes: multidomain anti-apoptotic proteins homologous in all 4 BH (BCL-2 homology)

domains; multidomain pro-apoptotic proteins (BAX, BAK) homologous in BH1, BH2 and BH3 domains; and BH3-only proteins, which all are pro-apoptotic and bind to the multidomain members (Danial & Korsmeyer, 2004). It has further been suggested that certain pro-apoptotic BH3-only proteins have a sensitizer function and sequester anti-apoptotic BCL-2 family members away from interactions with the multidomain pro-apoptotic proteins, whereas other BH3-only proteins are activators of the pro-apoptotic multidomain family members (Certo *et al*, 2006). Pro-apoptotic multidomain BAX and BAK, which are essential for apoptosis, homooligomerize upon activation (Certo *et al*, 2006), leading to release of mitochondrial apoptotic co-factors cytochrome *c* and Smac/DIABLO (Danial & Korsmeyer, 2004). Then cytochrome *c* is bound by Apaf-1, which forms Apaf-1 oligomers and recruits pro-caspase 9. Caspase 9 activation activates downstream caspases that execute apoptosis (Danial & Korsmeyer, 2004).

This work aimed to build a foundation for overcoming drug resistance from abnormal cell death regulation in leukaemias with t(4;11). Although few infant cases were included in prior paediatric studies (Maung *et al*, 1994; Coustan-Smith *et al*, 1996; Uckun *et al*, 1997), virtually all cases of paediatric ALL express detectable BCL-2 protein (Coustan-Smith *et al*, 1996). Because of the importance of specific regulators of apoptosis in different cancer cell types (Certo *et al*, 2006), and because BCL-2 was the critical anti-apoptotic protein for maintenance of B-lymphoblastic leukaemia in a conditional BCL-2 transgenic mouse (Letai *et al*, 2004), we investigated BCL-2 as a potential therapeutic target. First, baseline *BCL2* mRNA and/or protein expression was characterized in infant and paediatric leukaemias with t(4;11) or other *MLL* translocations or without *MLL* translocations. The finding of abundant *BCL2* mRNA and protein formed the basis to evaluate the effects of the pro-apoptotic *BCL2* antisense compound Genasense™ (Oblimersen Sodium, G3139; Genta, Incorporated, Berkeley Heights, NJ, USA) as a prototypic strategy for targeting apoptosis in cell lines with t(4;11) and similar abundant *BCL2* expression to the primary cases with this translocation. Evaluation of this agent, designed to decrease BCL-2 protein levels via selective *BCL2* mRNA degradation, also was of interest because of its clinical activity in refractory and relapsed adult B-cell malignancies (Waters *et al*, 2000; O'Brien *et al*, 2005) and acute leukaemias (Marcucci *et al*, 2003).

Materials and methods

The Institutional Review Board at The Children's Hospital of Philadelphia approved this research. Three cell lines derived from adult (RS4:11) (Stong *et al*, 1985) or paediatric (MV4-11 and SEM-K2) (Lange *et al*, 1987; Pocock *et al*, 1995) leukaemias with t(4;11), and total RNA ($n = 27$ cases) or protein ($n = 3$ cases) isolated from leukaemic marrow or peripheral blood mononuclear cells from diagnosis of infant/paediatric acute leukaemia cases were used for these studies. The patient

materials were archived at The Children's Hospital of Philadelphia ($n = 28$) or obtained from the Children's Oncology Group Leukaemia Cell Bank at the University of New Mexico ($n = 2$). The characteristics of some of the patients have been described before (Felix *et al*, 1997, 1998a,b; Raffini *et al*, 2002). The *MLL* translocations were identified and characterized or excluded by standard cytogenetics, Southern blot analysis, reverse transcription polymerase chain reaction (PCR) and/or panhandle PCR-based methods (Felix *et al*, 1997; Raffini *et al*, 2002; Robinson *et al*, 2006).

Western blot analysis of BCL-2 protein expression

Endogenous BCL-2 protein levels were measured in the RS4:11, MV4-11 and SEM-K2 cell lines and leukaemia cell lysates of three patients (two infants, one child) with ALL with t(4;11). The cells were washed with ice-cold phosphate-buffered saline (PBS; Invitrogen, Grand Island, NY, USA) and lysed in extraction buffer (50 mmol/l Tris-HCl, 150 mmol/l NaCl, 0.5% SDS, 1% sodium deoxycholate, 1% Nonidet P-40) containing a protease inhibitor cocktail (Roche, Indianapolis, IN, USA). Cell lysates were incubated on ice for 10 min, passed through a 27-gauge needle to shear the DNA, and centrifuged at 14 000 g for 20 min at 4°C. Supernatants were retained as total cellular proteins. Protein concentrations were determined using the Lowry method as per the manufacturer's protocol (BioRad, Hercules, CA, USA) using bovine serum albumin (Pierce, Rockford, IL, USA) as the calibration standard. Proteins were separated by 4–12% NuPAGE SDS-PAGE, and then transferred onto nitrocellulose membranes (Invitrogen). Membranes were blocked with 5% non-fat milk in Tris-buffered saline with 0.05% Tween-20 (TBST) for 1 h at room temperature. After adding anti-BCL-2 antibody (1:1000 dilution), the membranes were incubated overnight at 4°C. On the next day, the appropriate alkaline phosphatase-conjugated secondary antibody solution was added to the membranes followed by a 30-min incubation at room temperature. The membranes were washed extensively with wash solution and developed using chemiluminescent substrates (Western Breeze kit; Invitrogen). The membranes were stripped and hybridized with an anti- β -actin antibody to control for equal loading.

Quantitative real-time PCR analysis of BCL2 mRNA expression

Baseline *BCL2* mRNA expression levels were determined in the three cell lines and 27 infant/paediatric leukaemia cases with ($n = 15$) or without ($n = 12$) an *MLL* translocation (Table I). Random hexamer-primed first-strand cDNAs were synthesized from 1 to 10 μ g of total RNAs using a High Capacity cDNA Archive Kit (Applied Biosystems, Foster City, CA, USA). cDNA templates were analysed using an Assay-On-Demand kit (Applied Biosystems) for *BCL2*, and a Pre Developed TaqMan Assay Reagent kit was used for the 18S rRNA endogenous control (Applied Biosystems). Gene expression was quantified

Table I. Patient characteristics.

	MLL (15)	Non-MLL (12)
Age at diagnosis (years)		
<1	10	1
1–10	4	7
>10	1	4
Gender		
Male	6	8
Female	9	4
Acute lymphoblastic leukaemia		
Precursor B	8	5
	MLL-AFF1 (4)	
	MLL-MLLT1 (4)	
T cell	0	2
Acute myeloid leukaemia	7	5
	MLL-AFF1 (1)	
	MLL-MLLT3 (5)	
	MLL-MLLT1 (1)	

AFF1 has also been called AF-4; MLLT1 has also been called ENL; MLLT3 has also been called AF-9.

using the relative standard curve method with RS4:11 as the calibrator sample.

Real-time PCR analysis of BCL2 mRNA expression after G3139 or G3622 treatment

Genasense™ (Oblimersen Sodium, G3139; Genta, Incorporated, Berkeley Heights, NJ, USA) is an 18-mer phosphorothioate antisense oligodeoxynucleotide (ODN) that forms a DNA–RNA hybrid with the first six codons of the open reading frame of BCL2 RNA (Nicholson, 2000). G3622 (Genta) is the reverse polarity control sequence for G3139. RS4:11 cells (6×10^5) were plated in growth medium in triplicate in a six-well dish and exposed to 200 $\mu\text{mol/l}$ G3139 or G3622 for 24 h or reserved untreated. RNA was extracted using a RNeasy kit (Qiagen, Valencia, CA, USA). Random hexamer-primed first-strand cDNAs were synthesized from 10 μg of total RNAs using a High Capacity cDNA Archive Kit (Applied Biosystems) and 10 ng of cDNA templates were analysed using Assay-On-Demand kits (Applied Biosystems) for BCL2 and the GAPDH endogenous control gene. Gene expression was quantified using the comparative C_T method (Livak & Schmittgen, 2001).

Western blot analysis of BCL-2 protein levels after G3139 or G3622 treatment

BCL-2 protein modulation after treatment of RS4:11 cells with G3139 or G3622 was assessed by Western blot analysis. RS4:11 cells (6×10^5) were plated in growth medium in triplicate in a six-well dish and exposed to either 200 $\mu\text{mol/l}$ G3139 or G3622 for 48 h or reserved untreated. Proteins were extracted and visualized as above, except that total cellular proteins were separated on a 4–12% Bis-Tris gradient gel.

MTT assay of cell survival

Cytotoxicity of G3139 delivered without transfection reagent against the cell lines was determined using MTT [(3–4,5-dimethylthiazol-2-yl)-2,5-diphenyl tetrazolium bromide] assays of cell viability/proliferation (Pieters *et al*, 1990). Control ODNs used in MTT assays of single agent G3139 included the reverse polarity control sequence G3622 and a two-base mismatch sequence G4126 (5′-TCTCCCAGCA-TGTGCCAT-3′). Cells were plated in log-phase growth at 500 000 cells/ml (RS4:11 and SEM-K2) or 200 000 cells/ml (MV4-11) in media [RS4:11 and SEM-K2, RPMI1640 + 10% fetal bovine serum (FBS); MV4-11, Iscove's + 10% FBS] in a 96-well flat-bottom tissue culture plate (Becton Dickinson Labware, Franklin Lakes, NJ, USA). Twenty-four hours after plating, the cells were treated with vehicle or increasing concentrations of G3139 or cytotoxic drug alone, or increasing concentrations of cytotoxic drug combined with G3139 at a fixed concentration (three to six replicates per experiment per condition). The cytotoxic drugs examined were doxorubicin (ADR), cytosine arabinoside (ARAC), 6-thioguanine (6-TG), etoposide (VP16), methotrexate (MTX) and dexamethasone (DEX) (Sigma-Aldrich, St. Louis, MO, USA). MTT Cell Proliferation Assays (American Type Culture Collection, Manassas, VA, USA) were performed after 6 d of exposure. The background signal from media-alone controls was subtracted and the data were normalized to vehicle-treated cells [G3139, PBS; DEX, ethanol; other cytotoxic drugs, dimethyl sulfoxide (DMSO)] to determine the surviving fraction. All MTT experiments were performed at least twice. Additional MTT assays were conducted in RS4:11 cells on triple combinations with the G3139 concentration fixed at 5 $\mu\text{mol/l}$ and varying concentrations of VP16 and ARAC.

Pharmacostatistical modelling of drug interactions

The MTT assay data were analysed using a variation of the Loewe additivity drug interaction model (Greco *et al*, 1995), $d_x/D_x + d_y/D_y = I$, where D_x and D_y are doses of individual drugs required to exert the same effect as doses d_x and d_y used in combination (Greco *et al*, 1995). If the experimental product of this equation (Loewe combination index, I) = 1, then the interaction is additive; if <1, synergistic; if >1, antagonistic. The COMBITOOL™ program (version 2.001, Biocomputing Group, Leibniz Institute for Age Research, Jena, Germany) was used to generate three-dimensional scatter plots of the observed data from cytotoxic agents combined with G3139 compared to the response surface predicted from single agent experiments using the Loewe additivity equation (Dressler *et al*, 1999). The sigmoid Emax model, $E(d) = d^\mu/(\alpha^\mu + d^\mu)$, was applied to determine the parameters α (effective concentration at which 50% of the cells survive, EC_{50}) and μ (slope of the curve, Hill coefficient) for G3139, G3622 and cytotoxic drugs using the WINNONLIN (version 4.1) software program (Pharsight Corp., Mountain View, CA, USA). The zero-interaction response

surface for the drug combinations was simulated using a variation of the Loewe additivity equation:

$$d_A / \{ \alpha_A [E_{AB}^{LA} / (1 - E_{AB}^{LA})]^{1/\mu_A} \} + d_B / \{ \alpha_B [E_{AB}^{LA} / (1 - E_{AB}^{LA})]^{1/\mu_B} \} + \dots = 1,$$

where E_{AB}^{LA} is the zero interaction response surface, d_A and d_B are the concentrations for drugs A and B, α_A and α_B are the drug concentrations resulting in 50% cell death and μ_A and μ_B are the slope parameters describing the concentration–effect relationships for drugs A and B. Experimental concentration ranges for d_A and d_B were chosen to encompass the smallest doses of G3139 (delivered without transfection reagent) and the relevant cytotoxic drugs that showed activity in single agent MTT assays. The zero-interaction response surface of fixed concentration G3139 (5 $\mu\text{mol/l}$) combined with increasing concentrations of VP16 and ARAC together was derived by modifying the Loewe additivity equation to accommodate the experimental interaction of the triple combination.

Flow cytometry analyses of apoptosis

RS4:11 cells were plated in growth media at 500 000 cells/ml in log-phase growth in six-well dishes (Becton Dickinson Labware), exposed 24 h later to either vehicle (DMSO), ADR alone (10 nmol/l), G3139 alone (1 $\mu\text{mol/l}$), or a G3139-ADR combination, and harvested 24, 48 or 72 h after treatment. For flow cytometric quantification of active caspase 3, cells were washed and prepared for staining using Caltag Fix and Perm (Caltag Laboratories, Burlingame, CA, USA). Following permeabilization, the cells were stained with a phycoerythrin (PE)-conjugated monoclonal rabbit anti-active caspase-3 antibody (BD PharMingen, San Diego, CA, USA) and analysed on a FACSCalibur instrument using CELLQUEST™ software (BD Biosciences, San Jose, CA, USA). Ten thousand events were collected for each sample and the data were represented on dot plots with caspase-3 PE (FL2) on the X-axis and the cell counts (event frequency) on the Y-axis. Fractions of active caspase 3 positive cells in the different ungated treated cell populations were determined by comparison with the vehicle treated cells. Data were also plotted using light scatter dot plots with forward scatter on the X-axis and side scatter on the Y-axis for quality control.

For flow cytometric TUNEL experiments, cells were prepared as previously described with minor modification (Gorczyca *et al*, 1993; Douglas *et al*, 1998). Briefly, 10^6 cells were washed in staining buffer containing 3% FBS (HyClone, Logan, UT, USA) in PBS (Invitrogen) and prepared for staining by paraformaldehyde (Electron Microscopy Sciences, Hatfield, PA, USA) fixation (1%) and permeabilization with 0.1% Triton X-100 (Roche). Subsequently, DNA was labelled with Cy5-dUTP (Promega, Madison, WI, USA) with or without addition of TdT (Roche). Ten thousand events were collected for each sample

on a dual laser FACSCalibur instrument (BD Biosciences, San Jose, CA, USA). Data were analysed using CELLQUEST™ software and represented on dot plots. Parallel no-TdT controls for endogenous TdT prepared for each condition were always $\leq 2\%$. To determine percentages of apoptotic cells, forward light scatter was plotted on the X-axis and Cy-5-dUTP (FL4) on the Y-axis. A region marker was set using the parallel no-TdT control for each condition, and events falling within this region were considered apoptotic.

One-way ANOVA with Newman–Keuls post-test was used to determine *P*-values (PRISM 4.0) to ascertain if the results of different treatments in the flow cytometry experiments were different.

Cell-cycle analysis

RS4:11 cells were plated in growth media at 500 000 cells/ml in log-phase growth in six-well dishes (Becton Dickinson Labware) and exposed 24 h later to either vehicle (PBS) or G3139 (1, 10 or 100 $\mu\text{mol/l}$) and harvested 24, 48 or 72 h after treatment. Cells were washed in staining buffer (PBS containing 3% FBS) and prepared for staining by fixation in 2% paraformaldehyde and permeabilization in 0.1% Triton X-100. Cells were then incubated with propidium iodide (Invitrogen) on ice for 1 h and analysed by flow cytometry on a FACSCalibur instrument. Twenty thousand events were collected for each sample. Data were analysed using ModFit LT for Mac (Verity Software House, Topsham, ME, USA).

Results

Leukaemias with t(4;11) contain abundant BCL-2 protein and mRNA

The Western blot experiments demonstrated abundant anti-apoptotic BCL-2 protein levels in the cell lines RS4:11 (Stong *et al*, 1985), SEM-K2 (Pocock *et al*, 1995) and MV4-11 (Lange *et al*, 1987) and three primary infant/paediatric leukaemias with t(4;11) (Fig 1A). In addition to the anti-apoptotic 28 kD species, a pro-apoptotic BCL-2 cleavage fragment, which is derived from caspase cleavage of BCL-2 (Cheng *et al*, 1997), was detected in the MV4-11 cell line only (Fig 1A, left). Quantitative real-time PCR analysis of 27 primary infant/paediatric leukaemias (Table I) and the same cell lines suggested greater mean *BCL2* mRNA expression in the *MLL*-rearranged cases and the cell lines with t(4;11) than in the cases with *MLL-MLL1* or *MLL-MLL3* translocations and the ALL and acute myeloid leukaemia (AML) cases without *MLL* translocations (Fig 1B). However, there was variability, and sometimes substantial expression within each leukaemia subtype, although the sample size was limited. The cell lines with t(4;11) were used as models for further experiments since they expressed abundant *BCL2* mRNA and protein levels similar to primary leukaemia cases with t(4;11).

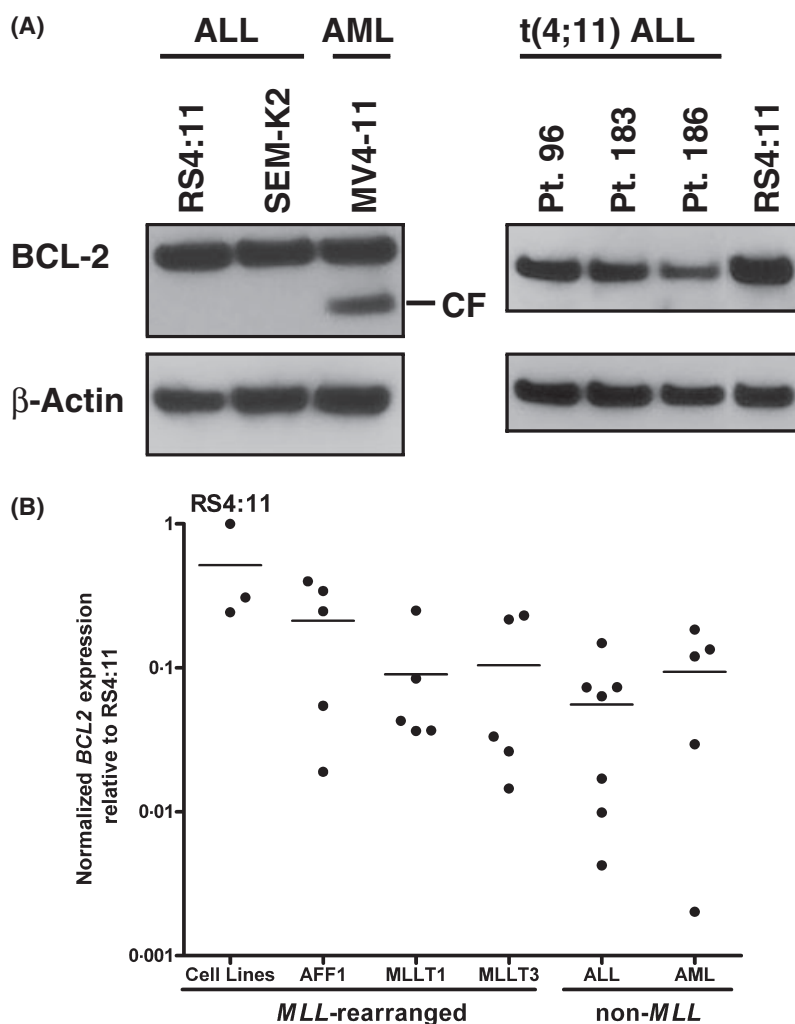


Fig 1. Endogenous *BCL-2* protein and mRNA levels in cell lines with t(4;11) and primary infant/paediatric leukaemias. (A) *BCL-2* protein expression was examined in 4–10 µg of total protein by Western blot analysis. Patient 96 was a child; Patients 183 and 186 were infants. A cleaved form of *BCL-2* protein (CF) also was detected in MV4-11 cells. β -actin antibody was used to verify equal protein loading. (B) *BCL2* mRNA expression was quantified by real-time PCR in RS4:11, MV4-11 and SEM-K2 cell lines, 15 *MLL*-rearranged (5 each *MLL-AFF1*, *MLL-MLLT3*, *MLL-MLLT1*) and 12 non-*MLL* (7 ALL, 5 AML) leukaemia cases. *BCL2* mRNA expression data was quantified by the relative standard curve method, normalized to the 18S rRNA endogenous control. Dots indicate individual cases; horizontal lines indicate mean of normalized *BCL2* transcript expression relative to RS4:11 within subtypes.

Table II. Normalized *BCL2* mRNA expression in RS4:11 cells treated with G3139 or G3622 relative to no treatment.

Treatment	<i>BCL-2</i> C_T (avg. \pm SD)	GAPDH C_T (avg. \pm SD)	ΔC_T (avg. <i>BCL-2</i> C_T –avg. GAPDH C_T)	$\Delta\Delta C_T$ (avg. ΔC_T –avg. ΔC_T None)	Normalized <i>BCL2</i> mRNA relative to untreated cells ($2^{-\Delta\Delta C_T}$)
None	22.85 \pm 0.08	17.09 \pm 0.09	5.75 \pm 0.16	0	1
G3622	33.22 \pm 0.24	26.92 \pm 0.38	6.31 \pm 0.19	0.56 \pm 0.19	0.68 (0.59–0.77)
G3139	50*	27.10 \pm 0.39	22.90 \pm 0.39	17.15 \pm 0.39	6.9 $\times 10^{-4}$

Results represent averages of 3 reactions per condition.

*No threshold cycle was detected after 50 cycles.

G3139 delivered without transfection reagent decreases BCL2 mRNA and protein expression in RS4:11 cells

Real-time PCR and Western blot experiments demonstrated reduced *BCL2* mRNA and protein expression in RS4:11 cells

treated with G3139, consistent with suppression of the intended target. A 24 h exposure to G3139 at 200 µmol/l completely abrogated *BCL2* mRNA expression and the difference was highly significant compared to the G3622 reverse polarity sequence control ODN (Table II). *BCL-2* protein was

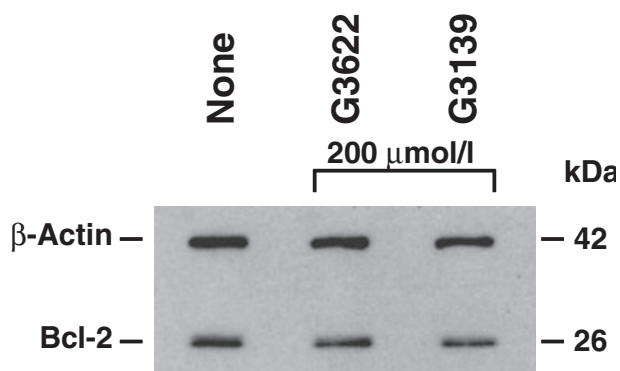


Fig 2. BCL-2 protein expression is reduced by G3139 treatment. Western blot analysis of BCL-2 protein compared to β -actin was performed on untreated cells or cells treated with 200 $\mu\text{mol/l}$ G3139 or G3622 for 48 h. Five microgram of total cellular protein were loaded per lane. Antibodies were mouse anti-human BCL-2 and mouse anti-human β -actin.

examined at 48 h because the reduction in protein was expected to follow the reduction in the mRNA. In RS4:11 cells exposed to 200 $\mu\text{mol/l}$ G3139 for 48 h, BCL-2 protein was appreciably reduced (Fig 2).

RS4:11 is the most sensitive of cell lines with *t(4;11)* to single-agent G3139

Treatment of RS4:11 cells with serial dilutions of the ODNs G3139, the reverse polarity sequence control G3622 or the 2-base *BCL2* mismatch sequence G4126 and determination of the surviving fractions indicated that G3622 was the more suitable control because G4126 exhibited an intermediate effect on cell viability/proliferation relative to G3139 and G3622 (data not shown). Therefore, the subsequent MTT assays of single agent G3139 utilized G3622 as the control ODN.

In representative MTT assays of *in vitro* cytotoxicity of G3139 and G3622, EC_{50} values of single agent G3139 were 7.8 ± 0.9 $\mu\text{mol/l}$ in RS4:11 cells, 91.7 ± 44.3 $\mu\text{mol/l}$ in MV4-11 cells, and 122.3 ± 15.4 $\mu\text{mol/l}$ in SEM-K2 cells (Fig 3). Although some lack of specificity is inherent in ODNs (Gewirtz *et al*, 1998), there was less cytotoxicity in each cell line with G3622 than with G3139. EC_{50} values of single-agent G3622 were 34.3 ± 0.1 $\mu\text{mol/l}$ in RS4:11 cells, 301.2 ± 104.5 $\mu\text{mol/l}$ in MV4-11 cells and 280.9 ± 16.5 $\mu\text{mol/l}$ in SEM-K2 cells (Fig 3). As a frame of reference, the mean steady state concentration (C_{ss}) of G3139 in a phase I adult trial dosing G3139 at 7 mg/kg/d for 7 d was 3.1 $\mu\text{g/ml}$ (c. 0.5 $\mu\text{mol/l}$) (Waters *et al*, 2000) and the mean C_{ss} and mean C_{max} of G3139 in a phase I paediatric trial dosing G3139 at 7 mg/kg/d for 7 d were 2.04 $\mu\text{g/ml}$ (c. 0.3 $\mu\text{mol/l}$) and 3.34 $\mu\text{g/ml}$ (c. 0.6 $\mu\text{mol/l}$) respectively (Rheingold *et al*, 2007). However, *in vitro* EC_{50} values and clinical exposures cannot be compared directly and *in vitro* intracellular ODN incorporation inherently is much lower when transfection reagent is not used (Gewirtz *et al*, 1998).

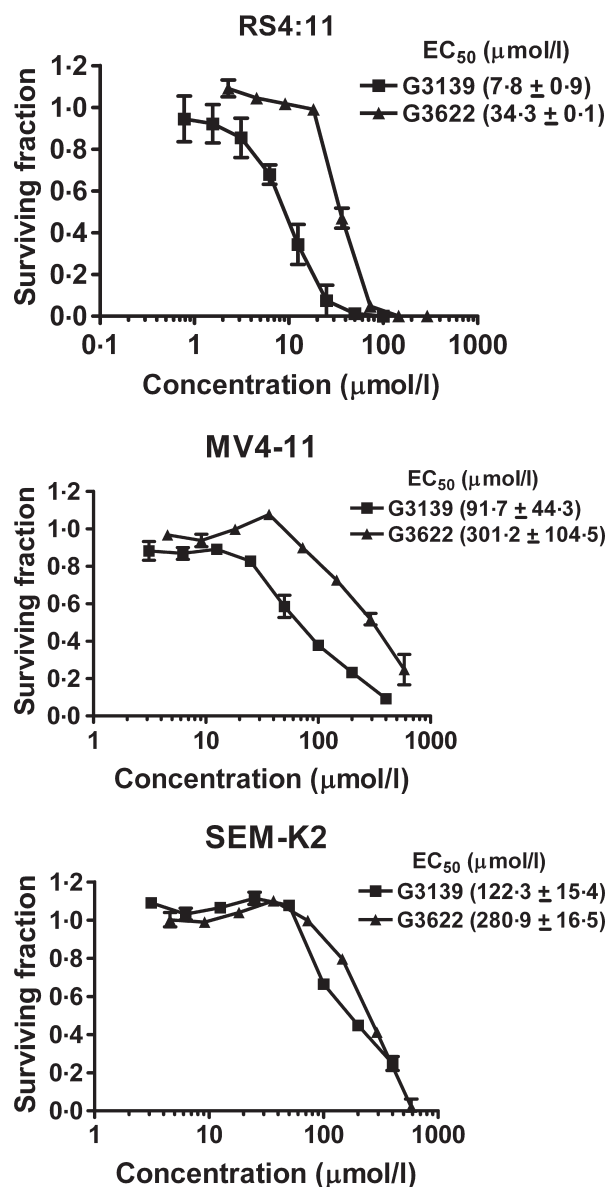


Fig 3. Single agent cytotoxicity of G3139 against cell lines with *t(4;11)*. Cells were plated in log-phase growth in a 96-well plate and treated with ODN 24 h later. Surviving fraction plots from representative MTT assays after a 6 d exposure to increasing concentrations of G3139 or reverse sequence control ODN G3622 for each cell line are shown. Experiments were performed three to four times. Surviving fractions were determined by normalization of the data to vehicle-treated cells after subtraction of background signal from media alone. Error bars represent the SEM for each data point consisting of six replicates. RS4:11 was most sensitive to G3139 of the cell lines tested. As expected (Gewirtz *et al*, 1998), G3622 showed some activity, though substantially less than G3139.

G3139 is synergistic with select cytotoxic agents against the RS4:11 cell line

RS4:11, the most sensitive of the cell lines to single-agent G3139 and the cell line in which *BCL2* expression was the highest, was the primary focus of experiments combining

G3139 with anti-leukaemia cytotoxic drugs. When the *in vitro* cytotoxicity of fixed concentrations of G3139 (1–20 $\mu\text{mol/l}$) combined with anti-leukaemia cytotoxic drugs over a range of concentrations was investigated by MTT assays, pharmacostatistical response surface modelling (Dressler *et al*, 1999) indicated that the lowest G3139 exposures tested (1 and 5 $\mu\text{mol/l}$) sensitized RS4:11 cells to the cytotoxic effects of ADR (Fig 4A), 6-TG (Fig 4B), VP16 (Fig 4C) and ARAC (Fig 4D), but not MTX (Fig 4E) or DEX (Fig 4F). Table III illustrates the EC_{50} values after single-agent cytotoxic drug exposures compared to the EC_{50} values after exposure to the cytotoxic drugs combined with 1 $\mu\text{mol/l}$ G3139. For each

synergistic cytotoxic drug-1 $\mu\text{mol/l}$ G3139 combination, the EC_{50} value is approximately one-half as compared to the cytotoxic drug alone. These data demonstrate that G3139 is synergistic with cytotoxic agents (ADR, 6-TG, VP16, ARAC) used in anti-leukaemia regimens at/near the no-effect concentration of G3139 alone. Furthermore, G3622 was not found to be synergistic with ADR in RS4:11 cells, indicating specificity of the observed interactions (data not shown).

Additionally, despite the higher single-agent EC_{50} of G3139 in MV4-11 cells, synergy also was suggested in this cell line when G3139 (10 and 50 $\mu\text{mol/l}$) was combined with VP16 or 6-TG (Fig 5).

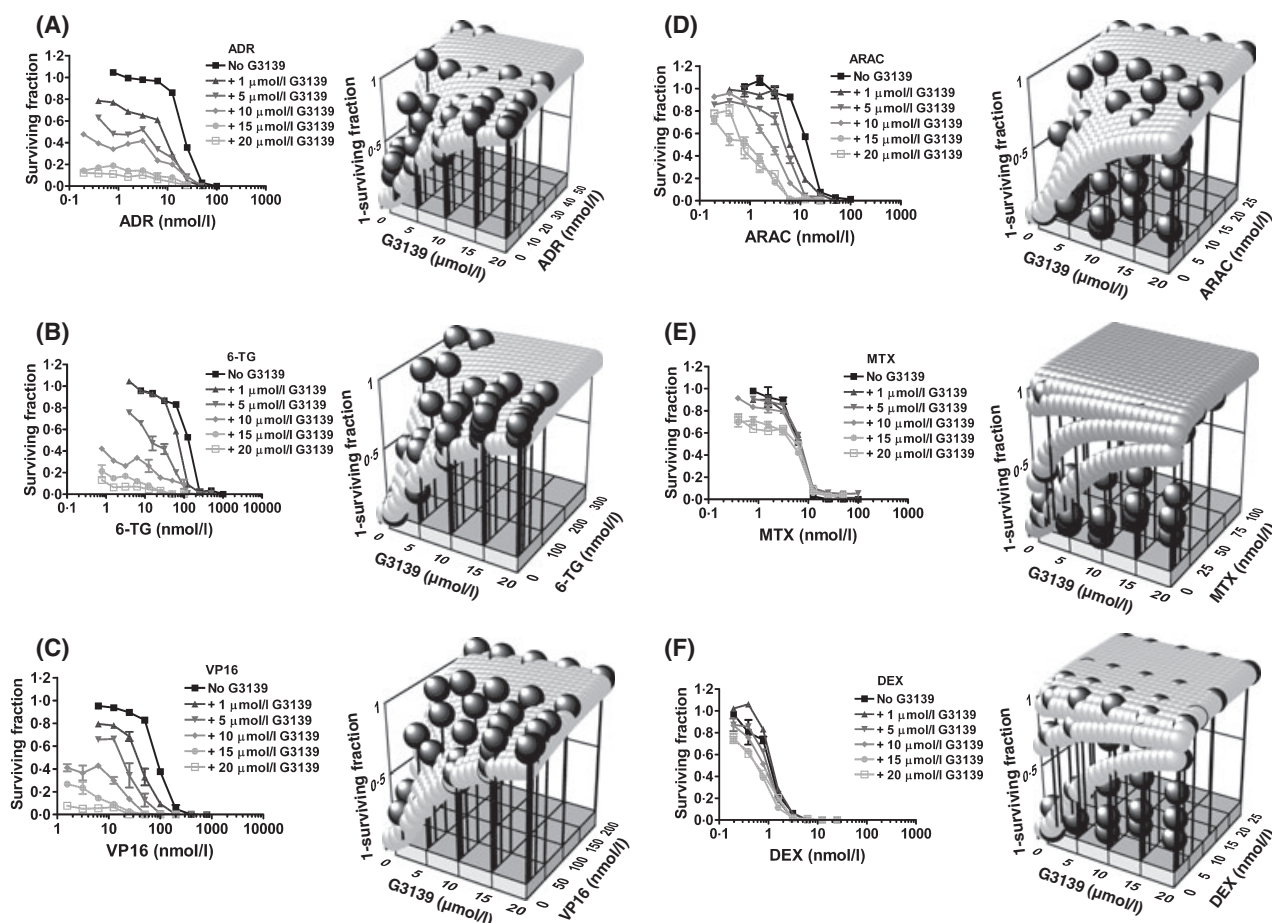


Fig 4. Combination experiments demonstrating synergistic effects of G3139 with select anti-leukaemia cytotoxic drugs in RS4:11 cells. (A–F, left) Surviving fraction plots from representative MTT assays performed after a 6 d exposure to increasing concentrations of cytotoxic drug alone or to increasing concentrations of cytotoxic drug combined with a fixed G3139 concentration (A, ADR; B, 6-TG; C, VP16; D, ARAC; E, MTX; F, DEX). Log-phase cells were treated with cytotoxic drug alone or combined with G3139 24 h after plating. Experiments were performed two to five times. Surviving fractions were determined by normalization of the data to vehicle-treated cells after subtraction of background signal from media alone. Error bars represent the SEM for each data point consisting of six replicates. (A–F, right) Representative response surface models (Dressler *et al*, 1999) showing three-dimensional scatter plot of the zero-interaction (additive) response surface derived from single-agent experiments on G3139 alone or cytotoxic drug alone (grey spheres) and observed data from MTT assays in which cytotoxic drug was combined with G3139 (black spheres). If the experimental combination effects are above the zero-interaction response surface, the combination is considered synergistic; if below the response surface, antagonistic; if on the response surface, additive (Dressler *et al*, 1999). Interactions achieved with (A) G3139–ADR, (B) G3139–6-TG, (C) G3139–VP16 and (D) G3139–ARAC, but not (E) G3139–MTX or (F) G3139–DEX were synergistic relative to the single agent profiles. Sigmoid Emax model was used to determine the EC_{50} and Hill coefficient for single agent dose responses (G3139: $\text{EC}_{50} = 7.8 \pm 0.9 \mu\text{mol/l}$, Hill coefficient = 1.6 ± 0.3 ; ADR: $\text{EC}_{50} = 21.2 \pm 0.4 \mu\text{mol/l}$, Hill coefficient = 3.4 ± 0.2 ; 6-TG: $\text{EC}_{50} = 121.5 \pm 14.5 \mu\text{mol/l}$, Hill coefficient = 2.5 ± 0.7 ; VP16: $\text{EC}_{50} = 84.3 \pm 5.9 \mu\text{mol/l}$, Hill coefficient = 2.7 ± 0.4 ; ARAC: $\text{EC}_{50} = 13.3 \pm 0.3 \mu\text{mol/l}$, Hill coefficient = 3.7 ± 0.4 ; MTX: $\text{EC}_{50} = 6.2 \pm 0.3 \mu\text{mol/l}$, Hill coefficient = 3.5 ± 0.6 ; DEX: $\text{EC}_{50} = 1.0 \pm 0.1 \mu\text{mol/l}$, Hill coefficient = 2.3 ± 0.4).

Table III. EC₅₀ values of single-agent cytotoxic drugs compared to cytotoxic drugs + 1 µmol/l G3139 in RS4:11 cells.

Drug	Single agent EC ₅₀	+1 µmol/l G3139
ADR	21.20 ± 0.37	11.00 ± 1.37
ARAC	13.29 ± 0.33	6.45 ± 0.47
6-TG	121.45 ± 14.54	66.53 ± 4.29
VP16	84.30 ± 5.90	34.39 ± 6.02
DEX	1.04 ± 0.10	1.21 ± 0.02
MTX	6.22 ± 0.29	6.36 ± 0.77

ADR, doxorubicin; ARAC, cytosine arabinoside; 6-TG, 6-thioguanine; VP16, etoposide; DEX, dexamethasone; MTX, methotrexate.

Anti-leukaemia cytotoxic agents are not administered alone when treating patients but in combinations. Additional triple agent combination MTT assays were conducted in RS4:11 cells with the G3139 concentration fixed at 5 µmol/l and varying concentrations of VP16 and ARAC. Response surface modelling of the triple combination showed that effective doses of

VP16 and ARAC were lower when G3139 was added, indicating that further synergy could be achieved by adding G3139 to a drug combination commonly used in patients (Fig 6).

G3139 potentiates ADR-induced apoptosis in RS4:11 cells

Since G3139 sensitized RS4:11 cells to the cytotoxicity of select anti-leukaemia chemotherapeutic agents, flow cytometric assays were performed to determine whether the observed synergy of the G3139-ADR combination in RS4:11 cells occurred through apoptosis. Caspase 3 target activation, an indicator of early-stage apoptosis (Patel *et al*, 1996), and TUNEL staining, an indicator of late-stage of apoptosis, were measured by flow cytometry. After exposure of RS4:11 cells to ADR (10 nmol/l) and G3139 (1 µmol/l) alone or in combination at concentrations <EC₅₀, there was no evidence of increased apoptosis as indicated by activated caspase 3 or increased TUNEL positivity at 24 or 48 h of exposure (data not

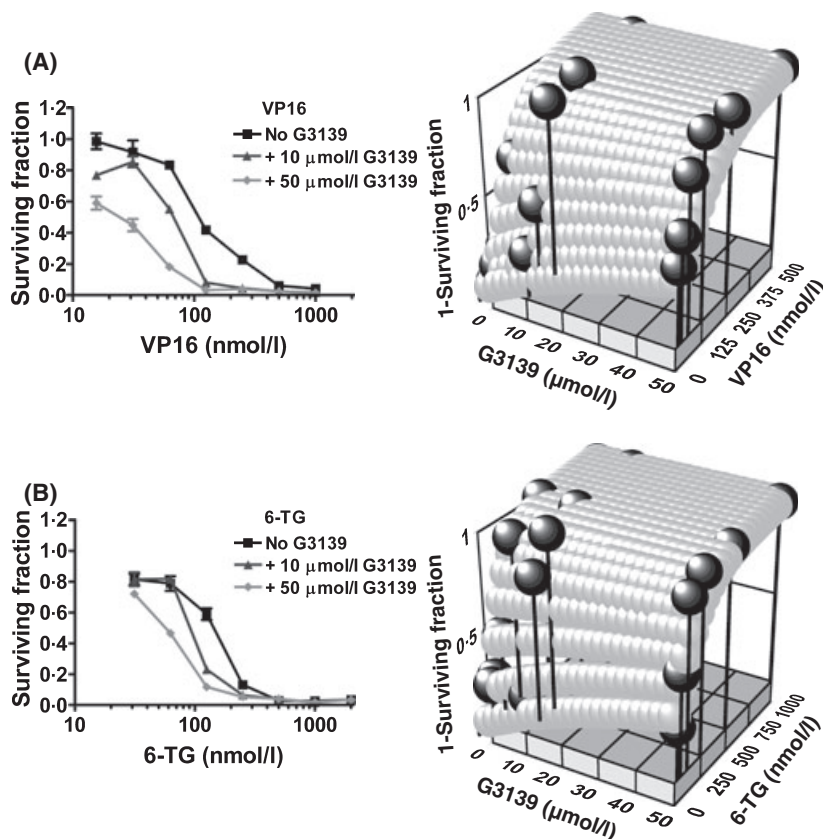


Fig 5. Combination experiments demonstrating synergistic effects of G3139 with select anti-leukaemia cytotoxic drugs in MV4-11 cells. (A–B, left) Surviving fraction plots from representative MTT assays performed after a 6 d exposure to increasing concentrations of cytotoxic drug alone or to increasing concentrations of cytotoxic drug combined with a fixed G3139 concentration (A, VP16; B, 6-TG). Experiment was performed twice. (A–B, right) Representative response surface models (Dressler *et al*, 1999) showing three-dimensional scatter plot of the zero-interaction (additive) response surface derived from single-agent experiments on G3139 alone or cytotoxic drug alone (grey spheres) and observed data from MTT assays in which cytotoxic drug was combined with G3139 (black spheres). Interactions achieved with (A) G3139–VP16 or (B) G3139–6-TG were synergistic relative to the single agent profiles. Sigmoid Emax model was used to determine the EC₅₀ and Hill coefficient for single agent dose responses (G3139: EC₅₀ = 91.7 ± 44.3 µmol/l, Hill coefficient = 1.0 ± 0.2; VP16: EC₅₀ = 112.1 ± 8.9 µmol/l, Hill coefficient = 2.2 ± 0.3; 6-TG: EC₅₀ = 126.2 ± 20.7 µmol/l, Hill coefficient = 1.9 ± 0.5).

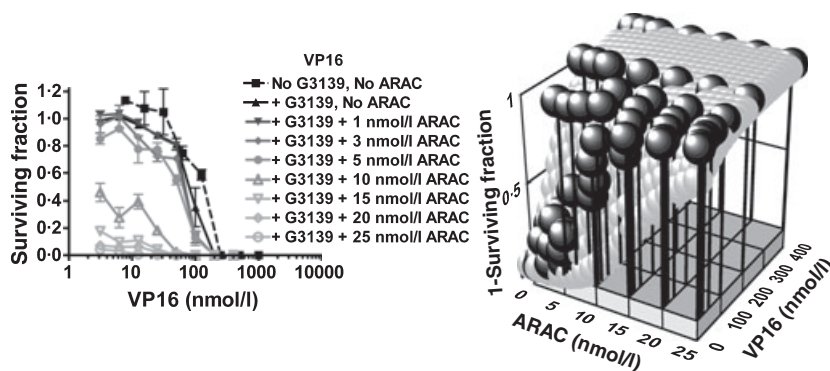


Fig 6. Synergistic interaction of G3139-ARAC-VP16 triple combination in RS4:11 cells. Log-phase cells were treated 24 h after plating with increasing concentrations of VP16 alone or combined with the fixed ARAC concentration indicated (range: 1–25 nmol/l), either without G3139 or with G3139 at fixed 5 μ mol/l concentration. MTT assays were performed 6 d after treatment. Representative experiment is shown. Experiment was performed twice. Surviving fractions were determined by normalization of the data to vehicle-treated cells after subtraction of background signal from media alone. Error bars represent the SEM for each data point consisting of three replicates from representative experiment. Three-dimensional scatter plot of data from MTT assays of G3139-VP16-ARAC triple combination (black spheres) compared to the Loewe additivity response surface of VP16 and ARAC (grey spheres), indicating synergistic interaction of the triple combination is at right (VP16: $EC_{50} = 127.0 \pm 16.4$ μ mol/l, Hill coefficient = 2.6 ± 0.8 ; ARAC: $EC_{50} = 17.5 \pm 0.4$ μ mol/l, Hill coefficient = 3.8 ± 0.3).

shown). However, by 72 h there was increased active caspase 3 positivity compared to vehicle (DMSO) in the cells exposed to ADR alone or G3139 alone. The fold increase in active caspase 3 positive cells over vehicle was maximal in cells treated with ADR and G3139 together (Fig 7A and B). Even though the fold increase in active caspase-3 positive cells over vehicle was greater with ADR alone than with G3139 alone ($P < 0.001$), the differences between the fold increase over vehicle with the G3139-ADR combination compared to either ADR alone ($P < 0.01$) or G3139 alone ($P < 0.001$) were significant (Fig 7B).

Similarly, in the flow cytometric TUNEL assays, exposure of RS4:11 cells for 72 h to low dose G3139 and ADR alone or together resulted in increased TUNEL staining over vehicle and the increase over vehicle was maximal with the G3139-ADR combination (Fig 7C and D). The increased TUNEL staining over vehicle was significantly greater with the combination compared to either ADR alone ($P < 0.05$) or G3139 alone ($P < 0.05$) (Fig 7D). In addition, the FSC vs. SSC light scatter plots demonstrated increases in side scatter and decreases in forward scatter typical of apoptotic cell populations, which paralleled the increases in active caspase-3 and TUNEL positivity (Fig 7). These data indicate that the synergistic cytotoxic G3139-ADR interaction was because of apoptosis.

G3139 exposure increases RS4:11 cells in S-phase

Since the anti-apoptotic effects of BCL-2 have been linked to cell-cycle retardation at the G_1/S transition (Deng *et al*, 2003), the effect of G3139 on cell-cycle progression was determined after exposure of RS4:11 cells to increasing concentrations of G3139. The flow cytometric assay demonstrated an increase in S-phase cells by 48 h after treatment (Fig 8). There was no

effect on cell cycle at 24 h after treatment and the increase in S-phase cells at 48 h diminished by 72 h after treatment (data not shown). The effect on S-phase progression also increased with increasing G3139 concentrations from 1 to 100 μ mol/l, indicating that the effect of G3139 on cell-cycle progression was both time and dose-dependent (Fig 8). The increased cell-cycle progression at the G_1/S transition is consistent with an effect of G3139 on the *BCL2* target transcript.

Discussion

We have shown that leukaemias with t(4;11) have abundant endogenous levels of *BCL2* mRNA and protein, providing an intrinsic cell survival mechanism for chemotherapy resistance. The high *BCL2* expression suggested that directly targeting *BCL2* RNA for degradation with G3139 might be an avenue to change the apoptosis threshold. Furthermore, the finding that anti-apoptotic *BCL2* mRNA and protein expression was similar in primary leukaemias and cell lines with t(4;11) provided the foundation for preclinical studies on this agent in cell lines. Others previously showed that the t(4;11) in several cell lines conferred resistance to stress-induced cell death upon serum deprivation (Kersey *et al*, 1998), possibly suggesting that abnormal cell death regulation contributed to their drug resistance. Additionally, increased *BCL2* expression was previously implicated in conferring the survival advantage of SEM-K2 cells in a xenograft model (Pocock *et al*, 1995). Moreover, targeting the intrinsic cell death pathway was rational because *BCL-2* overexpression prevents chemotherapy-induced apoptosis and nearly all cytotoxic anticancer drugs rely on the intrinsic apoptosis pathway (Reed, 2003). Even though the primary focus of this work was on reducing *BCL2* mRNA to increase chemosensitivity in leukaemias with t(4;11), *BCL2* expression is not exclusively a feature of *MLL* disease, as was

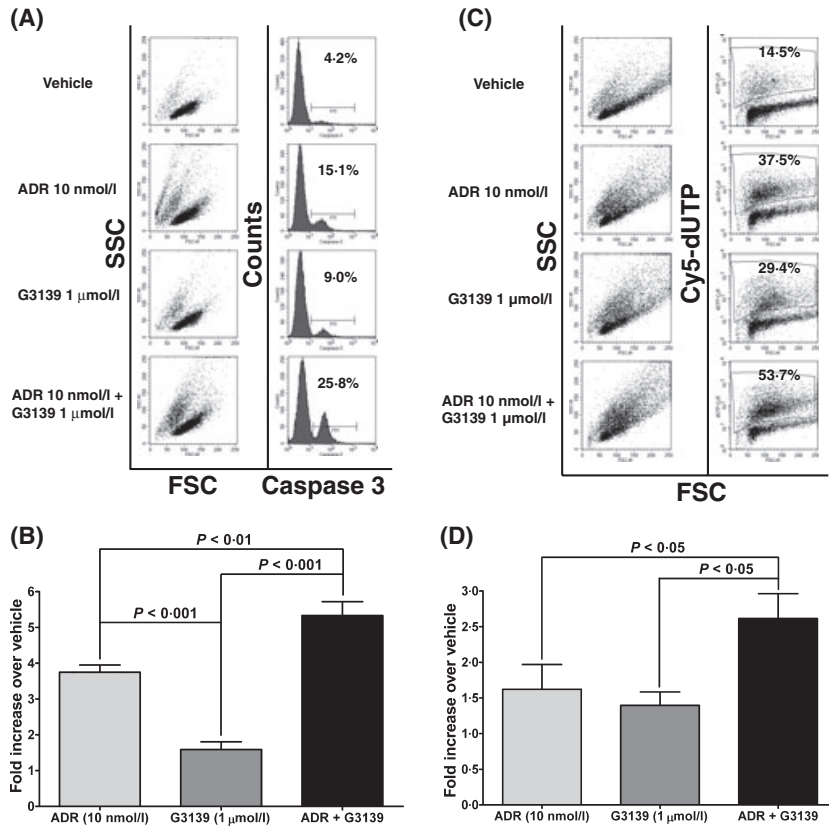


Fig 7. Flow cytometric assays of active caspase 3 and TUNEL staining demonstrating increased apoptosis in RS4:11 cells treated with G3139–ADR combination. Twenty-four hours after plating, log-phase RS4:11 cells were treated with vehicle, ADR (10 nmol/l), G3139 (1 μmol/l) or a combination of ADR and G3139 for 72 h. (A) Light scatter plot (left) and histogram (right) of pro- and active caspase 3 positive cell fractions in a representative experiment. Cells were gated by vehicle control (DMSO) where percentage of active caspase 3 was lowest. (B) Bar graph shows fold increase over vehicle (DMSO) of active caspase 3 positive cells after exposure to ADR (10 nmol/l), G3139 (1 μmol/l) or G3139–ADR combination averaged over four experiments (\pm SEM). (C) Light scatter plot and dot plot of Cy5-dUTP incorporation indicative of TUNEL positive cells in a representative experiment. Cells were gated by matched no TdT control, which was $<2\%$ positive for each condition. (D) Bar graph shows fold increase of TUNEL positive cells over vehicle (DMSO) after exposure to ADR (10 nmol/l), G3139 (1 μmol/l) or G3139–ADR combination averaged over five experiments (\pm SEM).

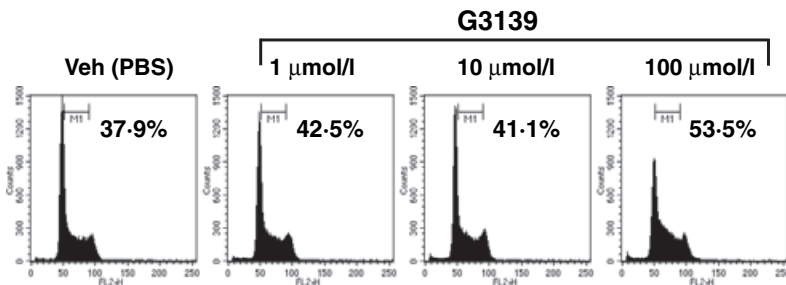


Fig 8. Flow cytometry analysis of G3139 effect on S-phase cell-cycle progression. Flow histograms of DNA content after PI staining of RS4:11 cells treated with vehicle (veh) or increasing concentrations of G3139. Representative experiment at 48 h, when effect of G3139 on cell cycle was maximal, is shown. Proportions of S-phase cells (region marker) for each condition were determined using ModFit LT for Mac. A higher proportion of S-phase cells is seen at the highest G3139 concentration. Experiment was performed twice.

described before (Maung *et al*, 1994; Coustan-Smith *et al*, 1996; Uckun *et al*, 1997). Similarly, variable and sometimes substantial *BCL2* mRNA expression levels also were detected in the other leukaemia subtypes studied here; however, these

results should be interpreted with caution because only a small number of cases were examined.

Many targeted strategies are emerging for silencing expressed genes and their effector proteins (Gewirtz *et al*,

1998; Letai *et al*, 2002; Reed, 2002, 2003; Hannon & Rossi, 2004). A 24 h exposure of RS4:11 cells to G3139 at 200 $\mu\text{mol/l}$ completely abrogated *BCL2* mRNA expression and the difference was highly significant compared to G3622. In addition, BCL-2 protein measured at the 48 h timepoint was appreciably reduced, indicating that *BCL2* mRNA and protein expression can be downregulated by G3139. These molecular effects of G3139 on *BCL2* mRNA and protein were measured at high concentrations to recognize the changes, not only because of the high endogenous BCL-2 protein, but also because of inherent limitations in delivering antisense *in vitro* when a transfection reagent is not used. However, cytotoxicity, effects on apoptosis and effects on cell cycle were observed at lower concentrations, indicating that lower G3139 concentrations are sufficient to modulate apoptosis and change the apoptosis threshold. Moreover, G3139 was cytotoxic to two different cell lines (RS4:11 and MV4-11) with t(4;11) and high levels of endogenous BCL-2 expression. In addition, G3139 at more subliminal concentrations potentiated the effects of particular cytotoxic drugs.

Preclinical models are essential to evaluate the benefit of combining molecularly targeted agents with anti-leukaemia cytotoxic drugs; however, previous preclinical pharmacodynamic activity data are limited regarding whether *BCL2* antisense ODNs are synergistic, additive or antagonistic with specific agents in specific disease conditions. Additionally, formal pharmacostatistical analyses of synergy are essential for a thorough understanding of interactions of molecularly targeted agents with different cytotoxic drugs. Here, a variation of the Loewe additivity equation (Greco *et al*, 1995; Dressler *et al*, 1999) was used to analyse G3139-cytotoxic drug interactions, and the results were incorporated into zero-interaction response surface models. While the RS4:11 cell line employed for many of the investigations was derived from a case of adult ALL (Stong *et al*, 1985), the t(4;11) translocation and, as shown in the present study, the BCL-2 protein levels were similar in primary paediatric/infant leukaemias and the RS4:11 cell line.

The effects of G3139 on cytotoxicity in RS4:11 cells was highly variable with the different anti-leukaemia chemotherapeutic agent combinations. Although some lack of specificity is inherent in ODNs from RNaseH cleavage of transiently formed duplexes with partial complementarity, aptameric (non-antisense) effects, such as ribosome binding causing protein synthesis inhibition or cytotoxicity from ODN degradation products (Gewirtz *et al*, 1998), there was substantially less cytotoxicity with the reverse polarity control ODN G3622 compared to G3139. In addition, G3139 exhibited synergistic cytotoxic interactions when combined with ADR, VP16, ARAC or 6-TG as evidenced by the response surface models (Dressler *et al*, 1999), which showed that effective doses were lower than projected from the single agent profiles. G3139 potentiated cytotoxicity in RS4:11 cells near/at the no-effect concentration of G3139 alone, which also is consistent with a synergistic interaction.

The *in vitro* studies were performed with G3139 concentrations from 1 to 20 $\mu\text{mol/l}$ recognizing that C_{ss} in adult and paediatric phase I trials dosing G3139 at 7 mg/kg/d were 3.1 $\mu\text{g/ml}$ (c. 0.5 $\mu\text{mol/l}$) (Waters *et al*, 2000) and 2.04 $\mu\text{g/ml}$ (c. 0.3 $\mu\text{mol/l}$) (Rheingold *et al*, 2007), respectively, and also that there are inherent *in vitro* cellular ODN uptake issues (Gewirtz *et al*, 1998) that preclude direct comparisons of *in vitro* and clinical dosing. Nonetheless, chemosensitivity and effects of G3139 on apoptosis occurred at the lowest G3139 concentration (1 $\mu\text{mol/l}$) tested. Even though the concentrations of G3139 used in the combination studies in the RS4:11 cell line were higher than those achieved in clinical trials, a transfection reagent was not used for drug delivery and it is not unexpected that somewhat higher *in vitro* concentrations were necessary to achieve these effects.

The VP16 and ARAC are often used together in anti-leukaemia regimens in patients. Pharmacostatistical response surface modelling demonstrated lower effective doses of VP16 and ARAC together when G3139 was added, indicating that further synergy could be achieved by adding G3139 to a drug combination used in patients.

Although both 6-TG and MTX both are anti-metabolites, synergy was observed with 6-TG but not MTX. It is of interest that G3139 exhibited synergy with ARAC because *MLL*-rearranged infant ALL is inherently more sensitive to ARAC than childhood ALL because of differential expression of genes encoding ARAC metabolizing enzymes (Stam *et al*, 2003). Further demonstration that apoptosis modulation enables ARAC dose reduction without changing efficacy in leukaemias with t(4;11) would be highly relevant because ARAC not only is an active cytotoxic agent, but also ARAC contributes significant regimen-related toxicities in the therapy of leukaemia in infants. In contrast, infant ALL manifests *in vitro* drug resistance to glucocorticoids (Pieters *et al*, 1998) and, in the RS4:11 cell line, the resistance was not overcome by G3139. This illustrates the necessity for preclinical activity data on each of the cytotoxic agents incorporated into anti-leukaemia regimens to evaluate which pro-apoptotic agent-cytotoxic drug combinations will be most beneficial.

Nonetheless, the experiments on synergy discussed above were conducted in the RS4:11 cell line derived from a case of adult ALL. The effects of G3139 on the MV4-11 cell line, derived from a case of childhood AML, strengthens the observation that G3139 is synergistic with select anti-leukaemia cytotoxic drugs in leukaemias with t(4;11). Even though the MV4-11 cell line was less sensitive to single-agent G3139 than the RS4:11 cell line, synergy still could be achieved when G3139 was combined with VP16 or 6-TG in MTT assays of MV4-11 cells near/at the no-effect concentration of G3139 alone.

There was additional heterogeneity in single-agent G3139 sensitivity among the cell lines tested. SEM-K2 was the least sensitive, even though there were differences in the IC₅₀ values between G3139 and G3622, as well as differences between G3139 activity compared to G3622 activity at lower concentrations

(Fig 3). The SEM-K2 cell line was derived from a case of paediatric ALL with t(4;11) at the time of relapse. *BCL2* was highly expressed in SEM-K2 cells, but there were probably other disease-related factors that made the cell line less responsive in addition to expression of the target transcript. Because many factors determine cell death regulation, it has been suggested that the principal effect of modulating *BCL2* mRNA is to tip the balance of the many factors to favour apoptosis (Nicholson, 2000). Elucidation of the differences in responsiveness to apoptosis modulation will be critical to advancing targeted agents directed at this pathway going forward.

The experiment addressing the effects of G3139 on cell cycle in RS4:11 cells is important because the anti-apoptotic effects of *BCL2* are linked to retardation of the G₁/S cell-cycle transition (Deng *et al*, 2003) and many anti-leukaemic cytotoxic drugs are cell-cycle dependent. The determination of the fractions of cells in G₀/G₁, S or G₂/M upon treatment of RS4:11 cells with G3139 as a single agent and the increased accumulation of cells in S phase of the cell cycle suggests that cell cycle may have had an impact on the increased chemosensitization when G3139 was combined with specific cell-cycle dependent cytotoxic drugs.

This study demonstrates that there is abundant *BCL2* mRNA and protein expression in paediatric/infant leukaemias with t(4;11). *BCL2* overexpression provides an important cell survival mechanism, and *BCL2* inhibition provides a potential avenue to achieving chemosensitivity in leukaemias with t(4;11). The synergy of specific G3139-anti-leukaemia cytotoxic agent combinations in two cell line models with the hallmark translocation and abundant *BCL2* mRNA and protein expression of acute leukaemia in infants suggests that the characteristic chemotherapy resistance can be overcome by targeting apoptosis regulation. Anti-apoptotic *BCL2* mRNA is a drugable molecular target in leukaemias with t(4;11) translocation.

Acknowledgements

We wish to thank Genta, Incorporated for providing G3139, G4126 and G3622 oligodeoxynucleotides. Some of the leukaemia samples utilized in this research were obtained from the Children's Oncology Group (COG) Leukaemia Cell Bank supported by COG Chair's Grant (CA98543) and the COG Cell bank grant (CA114766). This work was supported by Leukaemia & Lymphoma Society Translational Research Award no. 6205-02, Leukaemia & Lymphoma Society SCOR Grant no. 7372-07, the Joshua Kahan Foundation and Friends of the Joseph Claffey Fund.

References

Certo, M., Del Gaizo Moore, V., Nishino, M., Wei, G., Korsmeyer, S., Armstrong, S.A. & Letai, A. (2006) Mitochondria primed by death signals determine cellular addiction to antiapoptotic BCL-2 family members. *Cancer Cell*, **9**, 351–365.

Cheng, E.H., Kirsch, D.G., Clem, R.J., Ravi, R., Kastan, M.B., Bedi, A., Ueno, K. & Hardwick, J.M. (1997) Conversion of Bcl-2 to a Bax-like death effector by caspases. *Science*, **278**, 1966–1968.

Coustan-Smith, E., Kitanaka, A., Pui, C.-H., McNinch, L., Evans, W.E., Raimondi, S.C., Behm, F., Arico, M. & Campana, D. (1996) Clinical relevance of *BCL-2* overexpression in childhood acute lymphoblastic leukemia. *Blood*, **87**, 1140–1146.

Danial, N.N. & Korsmeyer, S.J. (2004) Cell death: critical control points. *Cell*, **116**, 205–219.

Deng, X., Gao, F. & May, W.S. Jr (2003) Bcl2 retards G1/S cell cycle transition by regulating intracellular ROS. *Blood*, **102**, 3179–3185.

Douglas, R.S., Pletcher, C.H. Jr, Nowell, P.C. & Moore, J.S. (1998) Novel approach for simultaneous evaluation of cell phenotype, apoptosis, and cell cycle using multiparameter flow cytometry. *Cytometry*, **32**, 57–65.

Dressler, V., Muller, G. & Suhnel, J. (1999) CombiTool – a new computer program for analyzing combination experiments with biologically active agents. *Computers and Biomedical Research*, **32**, 145–160.

Felix, C.A., Kim, C.S., Megonigal, M.D., Slater, D.J., Jones, D.H., Spinner, N.B., Stump, T., Hosler, M.R., Nowell, P.C., Lange, B.J. & Rappaport, E.F. (1997) Panhandle polymerase chain reaction amplifies MLL genomic translocation breakpoint involving unknown partner gene. *Blood*, **90**, 4679–4686.

Felix, C.A., Hosler, M.R., Slater, D.J., Parker, R.I., Masterson, M., Whitlock, J.A., Rebbeck, T.R., Nowell, P.C. & Lange, B.J. (1998a) MLL genomic breakpoint distribution within the breakpoint cluster region in de novo leukemia in children. *Journal of Pediatric Hematology/Oncology*, **20**, 299–308.

Felix, C.A., Walker, A.H., Lange, B.J., Williams, T.M., Winick, N.J., Cheung, N.K., Lovett, B.D., Nowell, P.C., Blair, I.A. & Rebbeck, T.R. (1998b) Association of CYP3A4 genotype with treatment-related leukemia. *Proceedings of the National Academy of Sciences of the United States of America*, **95**, 13176–13181.

Gewirtz, A.M., Sokol, D.L. & Ratajczak, M.Z. (1998) Nucleic acid therapeutics: state of the art and future prospects. *Blood*, **92**, 712–736.

Gorczyca, W., Gong, J. & Darzynkiewicz, Z. (1993) Detection of DNA strand breaks in individual apoptotic cells by the in situ terminal deoxynucleotidyl transferase and nick translation assays. *Cancer Research*, **53**, 1945–1951.

Greco, W.R., Bravo, G. & Parsons, J.C. (1995) The search for synergy: a critical review from a response surface perspective. *Pharmacological Reviews*, **47**, 331–385.

Hannon, G.J. & Rossi, J.J. (2004) Unlocking the potential of the human genome with RNA interference. *Nature*, **431**, 371–378.

Hilden, J.M., Dinndorf, P.A., Meerbaum, S.O., Sather, H., Villaluna, D., Heerema, N.A., McGlennen, R., Smith, F.O., Woods, W.G., Salzer, W.L., Johnstone, H.S., Dreyer, Z. & Reaman, G.H. (2006) Analysis of prognostic factors of acute lymphoblastic leukemia in infants: report on CCG 1953 from the Children's Oncology Group. *Blood*, **108**, 441–451.

Kersey, J.H., Wang, D. & Oberto, M. (1998) Resistance of t(4;11)(*MLL-AF4* fusion gene) leukemia to stress-induced cell death: possible mechanism for extensive extramedullary accumulation of cells and poor prognosis. *Leukemia*, **12**, 1561–1564.

Lange, B., Valtieri, M., Santoli, D., Caracciolo, D., Mavillio, F., Gemperlein, I., Griffin, C., Emanuel, B., Finan, J., Nowell, P. & Rovera, G. (1987) Growth factor requirements of childhood acute leukemia: establishment of GM-CSF-dependent cell lines. *Blood*, **70**, 192–199.

- Letai, A. & Scorrano, L. (2006) Laying the foundations of programmed cell death. *Cell Death and Differentiation*, **13**, 1245–1247.
- Letai, A., Bassik, M.C., Walensky, L.D., Sorcinelli, M.D., Weiler, S. & Korsmeyer, S.J. (2002) Distinct BH3 domains either sensitize or activate mitochondrial apoptosis, serving as prototype cancer therapeutics. *Cancer Cell*, **2**, 183–192.
- Letai, A., Sorcinelli, M.D., Beard, C. & Korsmeyer, S.J. (2004) Antia-poptotic BCL-2 is required for maintenance of a model leukemia. *Cancer Cell*, **6**, 241–249.
- Livak, K.J. & Schmittgen, T.D. (2001) Analysis of relative gene expression data using real-time quantitative PCR and the 2⁻[Delta Delta C(T)] method. *Methods*, **25**, 402–408.
- Marcucci, G., Byrd, J.C., Dai, G., Klisovic, M.I., Kourlas, P.J., Young, D.C., Cataland, S.R., Fisher, D.B., Lucas, D., Chan, K.K., Porcu, P., Lin, Z.P., Farag, S.F., Frankel, S.R., Zwiebel, J.A., Kraut, E.H., Balcerzak, S.P., Bloomfield, C.D., Grever, M.R. & Caligiuri, M.A. (2003) Phase I and pharmacodynamic studies of G3139, a Bcl-2 antisense oligonucleotide, in combination with chemotherapy in refractory or relapsed acute leukemia. *Blood*, **101**, 425–432.
- Maung, Z.T., MacLean, F.R., Reid, M.M., Pearson, A.D., Proctor, S.J., Hamilton, P.J. & Hall, A.G. (1994) The relationship between bcl-2 expression and response to chemotherapy in acute leukaemia. *British Journal Haematology*, **88**, 105–109.
- Nicholson, D.W. (2000) From bench to clinic with apoptosis based therapeutic agents. *Nature*, **407**, 810–816.
- O'Brien, S.M., Cunningham, C.C., Golenkov, A.K., Turkina, A.G., Novick, S.C. & Rai, K.R. (2005) Phase I to II multicenter study of oblimersen sodium, a Bcl-2 antisense oligonucleotide, in patients with advanced chronic lymphocytic leukemia. *Journal of Clinical Oncology*, **23**, 7697–7702.
- Patel, T., Gores, G.J. & Kaufmann, S.H. (1996) The role of proteases during apoptosis. *FASEB Journal*, **10**, 587–597.
- Pieters, R., Loonen, A.H., Huismans, D.R., Broekema, G.J., Dirven, M.W., Heynbrok, M.W., Hahlen, K. & Veerman, A.J. (1990) In vitro drug sensitivity of cells from children with leukemia using the MTT assay with improved culture conditions. *Blood*, **76**, 2327–2336.
- Pieters, R., den Boer, M.L., Durian, M., Janka, G., Schmiegelow, K., Kaspers, G.J.L., van Wering, E.R. & Veerman, A.J.P. (1998) Relation between age, immunophenotype and *in vitro* drug resistance in 395 children with acute lymphoblastic leukemia-implications for treatment of infants. *Leukemia*, **12**, 1344–1348.
- Pocock, C.F., Malone, M., Booth, M., Evans, M., Morgan, G., Greil, J. & Cotter, F.E. (1995) BCL-2 expression by leukaemic blasts in a SCID mouse model of biphenotypic leukaemia associated with the t(4;11)(q21;q23) translocation. *British Journal Haematology*, **90**, 855–867.
- Pui, C.H., Gaynon, P.S., Boyett, J.M., Chessells, J.M., Baruchel, A., Kamps, W., Silverman, L.B., Biondi, A., Harms, D.O., Vilmer, E., Schrappe, M. & Camitta, B. (2002) Outcome of treatment in childhood acute lymphoblastic leukaemia with rearrangements of the 11q23 chromosomal region. *Lancet*, **359**, 1909–1915.
- Pui, C.H., Sandlund, J.T., Pei, D., Campana, D., Rivera, G.K., Ribeiro, R.C., Rubnitz, J.E., Razzouk, B.I., Howard, S.C., Hudson, M.M., Cheng, C., Kun, L.E., Raimondi, S.C., Behm, F.G., Downing, J.R., Relling, M.V. & Evans, W.E. (2004) Improved outcome for children with acute lymphoblastic leukemia: results of total therapy study XIII B at St. Jude Children's Research Hospital. *Blood*, **104**, 2690–2696.
- Raffini, L.J., Slater, D.J., Rappaport, E.F., Lo Nigro, L., Cheung, N.K., Biegel, J.A., Nowell, P.C., Lange, B.J. & Felix, C.A. (2002) Panhandle and reverse-panhandle PCR enable cloning of der(11) and der(other) genomic breakpoint junctions of MLL translocations and identify complex translocation of MLL, AF-4, and CDK6. *Proceedings National Academy of Sciences United States of America*, **99**, 4568–4573.
- Reaman, G.H. (2003) Biology and treatment of acute leukemia in infants. In: *Treatment of Acute Leukemias: New Directions in Clinical Research* (ed. by C.-H. Pui), pp. 73–83. Humana Press, Totowa, NJ.
- Reaman, G., Zeltzer, P., Bleyer, W.A., Amendola, B., Level, C., Sather, H. & Hammond, D. (1985) Acute lymphoblastic leukemia in infants less than one year of age: a cumulative experience of the Children's Cancer Study Group. *Journal of Clinical Oncology*, **3**, 1513–1521.
- Reaman, G., Sposto, R., Senses, M., Lange, B., Feusner, J., Heerema, N., Leonard, M., Holmes, E., Sather, H., Pendergrass, T., Johnstone, H., O'Brien, R., Steinherz, P., Zeltzer, P., Gaynon, P., Trigg, M. & Uckun, F. (1999) Treatment outcome and prognostic factors for infants with acute lymphoblastic leukemia treated on two consecutive trials of the Children's Cancer Group. *Journal of Clinical Oncology*, **17**, 445–455.
- Reed, J.C. (2002) Apoptosis-based therapies. *Nature Reviews Drug Discovery*, **1**, 111–121.
- Reed, J.C. (2003) Apoptosis-targeted therapies for cancer. *Cancer Cell*, **3**, 17–22.
- Reed, J.C., Miyashita, T., Takayama, S., Wang, H.G., Sato, T., Krajewski, S., Aime-Sempe, C., Bodrug, S., Kitada, S. & Hanada, M. (1996) BCL-2 family proteins: regulators of cell death involved in the pathogenesis of cancer and resistance to therapy. *Journal of Cellular Biochemistry*, **60**, 23–32.
- Rheingold, S.R., Hogarty, M.D., Blaney, S.M., Zwiebel, J.A., Sauk-Schubert, C., Chandula, R., Krailo, M.D. & Adamson, P.C. (2007) Phase I trial of G3139, a bcl-2 antisense oligonucleotide, combined with doxorubicin and cyclophosphamide in children with relapsed solid tumors: a Children's Oncology Group Study. *Journal of Clinical Oncology*, **25**, 1512–1518.
- Robinson, B.W., Slater, D.J. & Felix, C.A. (2006) BglII-based panhandle and reverse panhandle PCR approaches increase capability for cloning der(II) and der(other) genomic breakpoint junctions of MLL translocations. *Genes, Chromosomes and Cancer*, **45**, 740–753.
- Stam, R.W., den Boer, M.L., Meijerink, J.P., Ebus, M.E., Peters, G.J., Noordhuis, P., Janka-Schaub, G.E., Armstrong, S.A., Korsmeyer, S.J. & Pieters, R. (2003) Differential mRNA expression of Ara-C-metabolizing enzymes explains Ara-C sensitivity in MLL gene-rearranged infant acute lymphoblastic leukemia. *Blood*, **101**, 1270–1276.
- Stong, R., Korsmeyer, S., Parkin, J., Arthur, D. & Kersey, J. (1985) Human acute leukemia cell line with the t(4;11) chromosomal rearrangement exhibits B lineage and monocytic characteristics. *Blood*, **65**, 21–31.
- Uckun, F.M., Yang, Z., Sather, H., Steinherz, P., Nachman, J., Bostrom, B., Crotty, L., Sarquis, M., Ek, O., Zeren, T., Tubergen, D., Reaman, G. & Gaynon, P. (1997) Cellular expression of antiapoptotic BCL-2 oncoprotein in newly diagnosed childhood acute lymphoblastic leukemia: a Children's Cancer Group Study. *Blood*, **89**, 3769–3777.
- Waters, J.S., Webb, A., Cunningham, D., Clarke, P.A., Raynaud, F., di Stefano, F. & Cotter, F.E. (2000) Phase I clinical and pharmacokinetic study of bcl-2 antisense oligonucleotide therapy in patients with non-Hodgkin's lymphoma. *Journal of Clinical Oncology*, **18**, 1812–1823.